Published in final edited form as:

FASEB J. 2021 July ; 35(7): e21747. doi:10.1096/fj.202100319RR.

The role of medial prefrontal cortex projections to locus ceruleus in mediating the sex differences in behavior in mice with inflammatory pain

Andrea Cardenas[1], **Alexander Papadogiannis**[2], **Eugene Dimitrov**[*]

[1]Center for the Neurobiology of Stress Resilience and Psychiatric Disorders, Rosalind Franklin University of Medicine and Science, 3333 Green Bay Road, North Chicago, IL 60064

[2]Chicago Medical School, Rosalind Franklin University of Medicine and Science, 3333 Green Bay Road, North Chicago, IL 60064, Tel: (860) 997-6818

Abstract

We tested the hypothesis that the cognitive impairment associated with inflammatory pain may result from dysregulation of the top-down control of locus ceruleus's (LC) activity by the medial prefrontal cortex (mPFC). Injection of complete Freund's adjuvant (CFA) served as a model for inflammatory pain. The CFA injection decreased the thermal thresholds in both sexes but only the male mice showed increased anxiety-like behavior and diminished cognition, while the females were not affected. Increased calcium fluorescence, a marker for neuronal activity, was detected by photometry in the mPFC of males but not in females with CFA. Next, while chemogenetic inhibition of the projections from the mPFC to the LC improved the object recognition memory of males with pain, the inhibition of the mPFC to LC pathway in female mice produced anxiolysis and spatial memory deficits. The behavior results prompted us to compare the reciprocal innervation of mPFC and LC between the sexes. We used an anterograde transsynaptic tagging technique, which relies on postsynaptic cre transfer, to assess the innervation of LC by mPFC efferents. The males showed a higher rate of post-synaptic cre transfer into LC neurons from mPFC efferents than the females. And vice versa, a retrograde tracing experiment demonstrated that LC to mPFC projection neurons were more numerous in females when compared to males. In conclusion, we provide evidence that subtle differences in the reciprocal neuronal circuit between LC and mPFC may contribute to sex differences associated with the adverse cognitive effects of inflammatory pain.

[*](corresponding author) Center for the Neurobiology of Stress Resilience and Psychiatric Disorders, Rosalind Franklin University of Medicine and Science, 3333 Green Bay Road, North Chicago, IL 60064, Tel: (847) 578-8364, eugene.dimitrov@rosalindfranklin.edu.

Authors Contributions

Study design by E.D., data acquisition and data analysis by A. C. and A. P. under supervision by E.D. Manuscript draft by E. D. with editing contributions by A. P. The work is supported by NIH grant R01MH105528 to E.D.

Conflict of interest

The authors declare that there are no financial or other benefits that might lead to conflict of interest.

Introduction

Pain is a multidimensional experience characterized by sensory, affective and cognitive components. The different pain modalities are conveyed and regulated through different but interacting CNS circuits and pain induced changes in the activity of these circuits may lead to pain-associated anxiety, depression and cognitive impairment (1). The central role of the mPFC for development of mental comorbidity associated with pain is well known (2). Pain drives the reorganization of local connectivity, alters the neuronal activity and affects the mPFC top-down regulation of lower brain centers, including loss of control over the descending pain inhibitory system (2–4). The descending modulation of pain relies on serotonin and norepinephrine (NE) for suppression of ongoing pain at spinal level and maladaptive changes in the system bring about pain chronification and pain-associated comorbidities (3–5).

In addition to pain inhibition, the NE modulatory functions include an array of specific adaptive behaviors, such as arousal, attention, mood, learning and memory (6–8). NE also modulates a range of autonomic functions namely heart rate, blood pressure and stress response (9–11). The main source for NE in the CNS is LC, which supplies NE not only to forebrain structures but also sends projections to the dorsal horn of the spinal cord for control of the nociceptive sensory input into CNS (12). The present view of LC organization is that the nucleus consists of discrete functional units that respond to a diverse range of stimuli and send out their efferents in region-specific arraignment (13–16). Different pain models in animals showed that while increased nociceptive input to the nucleus activates LC, protracted chronic pain tends to deactivate the nucleus in male rodents (17–20). Interestingly, detailed analysis of the LC anatomy and functions found an array of sexually dimorphic features such as cell number, dendritic length and complexity, and cell response to stimulation (21). The LC receives ample innervation from a number of brain structures, such as hypothalamus, amygdala, dorsal raphe and tegmentum to name a few but the mPFC is the only cortical region with projections to LC (22).

The mPFC is considered the main hub for cognitive functions including memory processes, goal-oriented behavior and impulse control (23) but it is also a control center for autonomic regulation (24, 25) and pain processing (26). The mPFC projections to brain stem structures including LC are essential for an array of cortical functions. Electrophysiological studies describe the direct mPFC projections to LC as excitatory (27) or as inhibitory via local interneuronal input (28). The mPFC to LC pathway is implicated in effort-related arousal, which finds expression in the pupil dilation during intense memorization (29). Additionally, the mPFC projections to the ventrolateral periaqueductal gray (vlPAG) are integrative part of the descending pain modulatory system and inhibition of the mPFC to vlPAG projections by pain causes decrease of NE and serotonin release in the spinal cord, thus augmenting the nociceptive input (30). There are noticeable similarities between the effects of different pain models on the activity of both mPFC and LC. While acute pain tends to activate the mPFC (31), chronic pain leads to inhibition of the mPFC (30). Similarly, various pain models demonstrate both, increased or decreased activity in the LC, a discrepancy which very likely stems from the duration of the painful injury (32). Furthermore, reports show increased expression of NE fibers in the mPFC and direct impairment of attention by NE release in the

mPFC after sciatic nerve injury (33, 34). However, the effects of inflammatory pain on the top-down regulation of LC by mPFC efferents and the subsequent changes in animal cognition remain unexplored.

Knowing that the inflammatory pain activates mPFC projections and that the mPFC regulates the activity of sexually dimorphic LC, which in turn, modulates an array of cognitive functions, we set forward experiments to investigate the effects of inflammatory pain on the cognitive performance of mice. We compared the behavior consequences of CFA injection in mice and aligned the behavior results with sex differences in the reciprocal connections between mPFC and LC.

Materials and Methods

Animals.

Outbred CD-1 mice of both sexes were purchased from Charles River Laboratories and were group housed at 10/14 hours light/dark daily cycle. The CD1 strain was chosen following the recommendations made by Mogil at al. that outbred mice are much less predisposed to abnormal behavior and that use of outbred mice improves reproducibility in pain research (35). The behavior experiments were conducted during the light cycle and were preceded by at least an hour of acclimatization to the specialized behavior testing room. All experiments and stereotaxic surgeries were carried out in accordance with the National Research Council Guide for the Care and Use of Laboratory Animals (National Academies Press, 2011) and the guidelines of the Animal Care and Use Committee at Rosalind Franklin University of Medicine and Science.

Stereotaxic Surgeries and Viral Injections.

The surgeries were performed under isoflurane anesthesia following an aseptic technique. The mice were placed in Stoelting stereotaxic frame after induction with gas anesthesia and 1 mm holes were drilled through the exposed skull. An air-tight Hamilton syringe with a 32-gauge needle was lowered into the brain with coordinates 1.8 mm, ± 0.4 mm and - 2.2 mm in respect to bregma for mPFC injections and with coordinates – 5.4 mm, ± 0.8 and – 3.5 mm to bregma for injections into LC. The viral injections were done by an infusion pump (Micro syringe pump, World Precision Instruments) at rate of 1.5 nl /second. The needle was withdrawn slowly 5 minutes after the injection. The wounds were closed with clips and analgesia with flunixin (2mg/kg) and fluids provided for the next three days. For photometry experiments, AAV_5.Syn.GCaMP6f.WPRE.SV40, titer ≥ 7×10^{12} (Addgene, 100837) in volume 100 nl was injected into the right mPFC. For chemogenetic experiments, 200 nl of the Cre activated $pAAV_5$-CaMKII-hM4D(Gi)-mCherry, titer ≥ 3×10^{12}, (Addgene, 50477) was injected bilaterally into the mPFC, while 100 nl of the retrograde rAAV-CAG-eGFP-F2A-Cre, titer ≥ 1×10^{12}, (NINDS Viral Production Core Facility) was injected bilaterally into the LC. The anterograde pENN.AAV_1.hSyn.cre.WPRE.hGH, titer ≥ 1×10^{13} (Addgene, 105553) was injected into the mPFC, while 200 nl of the cre-switch pAAV-Ef1a-DO-DIO-TdTomato-EGFP-WPRE-pA, titer ≥ 1×10^{13} (Addgene, 37120) was injected into LC in order to assess the mPFC innervation of LC by anterograde transsynaptic tagging (36, 37). The cre-switch pAAV-Ef1a-DO-DIO-TdTomato-EGFP-WPRE-pA changes the expression of the

default tdTomato (cre-off) to EGFP (cre-on) expression when activated by cre recombinase (38). The projections of LC to mPFC were evaluated by injection of 200 nl of the retrograde pENN.AAV.hSyn.HI.eGFP-Cre (titer ≥ 4.3×10^{12}, UPenn Vector core) into the right mPFC.

Injection of Complete Freund's Adjuvant (CFA) and Nociceptive Testing.

The rodent model of inflammatory pain includes an injection beneath the footpad of small volume of sterile CFA emulsion (39). CFA emulsion was purchased from Sigma, catalog number F5881. Only a single injection of 0.02 ml was applied to the left hind paw of each mouse. The substance causes local inflammatory response expressed as swelling and redness of the skin, which lasts from 10 to 12 days. The control mice were injected in the same manner with sterile saline.

Thermal sensitivity was assessed by Hargreaves test using a Heat-Flux Radiometer (Ugo Basile). Mice were placed in individual compartments on a platform with a glass floor. A beam of infrared light was aimed at the lateral side of the hind paw of mice when they had a paw firmly pressed against the glass. The heated glass floor produces a continuous rise in temperature of the paw until the pain threshold of the animal is reached and the animal withdraws the paw from the stimulus, which is automatically detected by the device. Pain threshold was determined by measuring the length of time that the radiant heat is applied, that is the latency of the paw withdrawal response of the animal (paw withdrawal latency). The intensity of the radiant heat was adjusted to a level to produce a paw withdrawal response at ~ 4 seconds with a cutoff time of 10 seconds. The average of three readings taken over an hour was used to determine the reaction latency to the heat.

Wireless Fiber Photometry of Calcium Transients.

The fiber photometry allows detection of Ca^{2+} transients in neuronal populations by measuring changes in the fluorescent intensity produced by a Ca^{2+} biosensor. Uprising of the intracellular Ca^{2+} induces fluctuations in the fluorescent signal, which corresponds with the neuronal activity in real time (40). The viral construct $pAAV_5$.Syn.GCaMP6f, titer $\geq 7 \times 10^{12}$ (Addgene, 10837) was injected in volume 100 nl into the right mPFC following the surgical technique and coordinates already described above. After three weeks, a fiber optic cannula, fiber core 400 μm/ NA 0.39, length 3 mm (Amuza Inc.) was lowered into the mPFC and secured to the skull with dental cement and three bone screws. The behavior experiments were conducted 7 to 15 days after the cannulations while mice were habituated to the equipment by wearing a dummy headstage. At the day of the experiment, a headstage transmitter was attached to the cannula. After adjusting the power of emitted light and stabilization of the signal, the mice were placed on Elevated O-maze for 5 minutes. The wireless headstage device (TeleFipho, Amuza Inc.) emits LED generated blue light at 470 nm, which is adjustable for power between 10 to 300 μW, while its photodiode detects green light with wavelength 500 – 550 nm at rate 100 Hz. The transmitter signal is sent to a digital receiver and recorded by Amuza software. We used the same software for analysis of the photometric traces. First, we measured the median baseline fluorescent signal for the entire 5 minutes of recordings and calculated the standard deviation (SD) of the baseline signal. Next, every positive deflection with intensity higher than 5 SD from baseline fluorescence was measured and the changes in fluorescent intensity were Z-scored using the formula (F_{sig}

– F_0)/F_{SD} where F_{sig} is the maximum amplitude of the measured fluorescent signal, F_0 is the fluorescence right before the measured signal and F_{sd} is the SD of the baseline fluorescence (41). The photometric recordings were performed once before CFA injection and 8 days after CFA injection and the traces of Ca^{2+} fluorescence were compared by within-subject analysis.

Behavior Tests.

The behavior tests were conducted from the 6th to the 10th post CFA-injection day in a specific order or Elevated O-Maze, Y-Maze Spontaneous Alternations, Novel Object Recognition followed by Puzzle test. A cohort of twenty to thirty mice was tested in a single experiment and the behavior tests were repeated 2 to 3 times, each time with a new cohort.

O-Maze.

The test equipment included a standard O-maze platform for mice with two open and two closed quadrants (Stoelting Co.), located in an isolated compartment of the behavior room. The mice were placed in any one of the open quadrants and their behavior was recorded for 5 minutes by a ceiling camera. Each video record started at the moment when the mouse first entered a closed quadrant. The anxiety like behavior was assessed from the video records, where the time spent in the open quadrants (the entire body of the mouse is in the open quadrant) was calculated as a percent of the total time on the maze.

Y-Maze Spontaneous Alternations.

This is a behavioral test based on the rodents' propensity to explore new environments. Rodents typically prefer to investigate a new arm of the maze rather than returning to one that was previously visited. We used a Y-shaped maze with three opaque plastic arms at a 120° angle from each other. After introduction to the center of the maze, the animal is allowed to freely explore the maze for 5 minutes. Over the course of multiple arm entries, the animal should show a tendency to enter a less recently visited arm. An entry occurs when all four limbs are within the arm. The number of arm entries and the number of triads are video recorded in order to calculate the percentage of correct alternations.

Novel Object Recognition Test (NOR).

The NOR paradigm starts with habituation of the mice to the testing arena, than the animals are placed in a testing arena with two similar objects for five minutes, return to their home cage for an interval of 3 hours and then returned to the testing arena with a copy of one of the original objects and a novel object. The session is video recorded and the amount of time investigating each of the objects is automatically measured by Any maze tracking software. The test provides a measure of the animal's memory for the previously investigated object (recognition memory). The used objects were impermeable plastic labware (e.g. test tube holders) that were easy to clean and sanitize.

Evaluation of Problem-Solving Ability.

The rodent mPFC plays an essential role in goal-oriented behavior. The puzzle test evaluates the ability of mice to solve a problem and relies on the natural rodent avoidance of bright

open spaces (42, 43). We used a simplified protocol of the published Puzzle test by combining a five-minute habituation phase followed by a problem-solving phase with a single obstacle. A well-lit, wide-open compartment was connected by a narrow tunnel to a smaller, dark compartment. The mice were placed in the open compartment and allowed to explore the apparatus for five minutes. After crossing the tunnel a few times, the mice uniformly entered and remained in the dark compartment. The animals were briefly removed from the box and a plug made of paper, which the mice could easily pull or push out of the tunnel, was used to block the entrance to the tunnel. The mice were returned to the open compartment and the time they needed to remove the plug and enter the dark compartment was measured.

Drugs.

Clozapine N-Oxide (CNO) (Tocris), an inert compound and ligand for the DREADD receptors, was injected intraperitoneally in dose 1mg/kg. The half-life of the small CNO dose used here is less than 2 hours and without any substantial metabolism back to its parent compound clozapine (44). The mice were randomly assigned to control and experimental groups and their group assignment was changed after each behavior tests. One hour before testing the mice in the experimental group received a CNO injection. The next day, the same group was used as a control and again as a CNO group on the following day. Therefore, the CNO injections in the same animals were separated by 48 hours.

Immunohistochemistry.

Mice were euthanized 24 hours after last behavior test, or the eleventh day after the CFA injection with an i.p injection of pentobarbital sodium (Vedco Inc.) and perfused transcardially with 0.01M phosphate buffered saline (PBS) followed by 4% paraformaldehyde in PBS. The collected tissue was sectioned into 40 μm thick coronal sections using Leica vibrotome.

The brain sections were washed with 0.01M PBS, incubated in 3% H_2O_2 for 15 minutes, again washed with 0.01M PBS, and then incubated in a blocking solution (0.01M PBS, 0.05% Triton X-100, 3% normal donkey serum) for 2 hours at room temperature. Then the sections were incubated with primary antibodies diluted in the same blocking solution at 4°C for 48 hours on rotating platform. The dilutions of primary antibody were 1:10K rabbit against c-Fos (anti-c-Fos; catalog 2250; Cell Signaling Technology), 1:2K chicken antibody to mCherry, (anti-mCherry, catalog CPCA-mCherry, EnCor Biotechnology Inc.), 1:1K sheep anti-TH (catalog 2026, Phosphosolutions), mouse anti-NET (norepinephrine transporter, catalog 1447, Phosphosolutions) and rabbit anti-GFP (catalog 10362, Invitrogen).

Following incubation with the primary antibody, sections for c-Fos and TH were incubated with the corresponding biotinylated secondary antibodies (Jackson ImmunoResearch Inc.), 1:2K dilution for 2 hours, followed by incubation in avidin-biotin complex (ABC kit, Vector Laboratories) for 1 hour at room temperature. The fluorescent signal was developed by incubation for 12 minutes in 20 nmol of tyramide conjugated Alexa Fluor 594 (c-Fos) or Pacific Blue (TH) fluorescent dyes. The rest of the immunostaining experiments were

completed by incubation of the sections with secondary antibodies conjugated to Alexa 488 or Alexa 594 in dilution 1:400 for 4 hours at room temperature.

Microscopy.

The immunostained brain sections were assessed by epifluorescent Leica DM5500 microscope equipped with CMOS camera. Coded microscopic slides containing at least six brain sections per animal were used to quantify the c-Fos, GFP and mCherry expressing cells in the LC. The atlas-matched brain sections covered the pontine region at three bregma levels, − 5.3, − 5.4 and − 5.6 mm to bregma. The multichannel images were split into single channel images and the individual cells were marked with the ImageJ multi-point tool. The colocalization was established by merging the single channels with already marked cells. The number of c-Fos cells was averaged per bregma level and subsequently pooled together for each animal with a complete set of sections. The number of cells expressing the viral markers GFP and mCherry and their colocalization with TH positive neurons was also averaged for each bregma level.

Statistical analysis.

The main goal of this study is to compare the behavioral effects of inflammatory pain between the sexes or to compare two independent variables, pain and sex, which led us to use Two-way ANOVA followed by Tukey's post hoc analysis for all behavior experiments, while mixed-effects ANOVA was used to compare the development of thermal hypersensitivity over time after the CFA injection. The fiber photometry results were analyzed by paired T-test, while the number of labeled cells in our tracing studies was compared by non-paired T-test. ROUT method with Q set at 1 was used to identify and exclude statistical outliers before subsequent analysis. All data are presented as mean ± SEM and analyzed with Graph Prism 8 software. The accepted level of significance was $P < 0.05$ in all tests.

Results

Inflammatory pain alters the behavior only of male but not female mice

The CFA injection is a well-established model for inflammatory pain in rodents. Inoculation of CFA into the foot pad of a laboratory animal reliably produces hyperalgesia (an increased response to noxious stimuli), which begins a few hours after the injection and continuous for to 2 weeks. The CFA nociception is triggered by mechanisms of peripheral and central sensitization with minimal effect on rodent mobility and overall health. In our hands, injection of 20 µl CFA into the plantar surface of the hind paw decreased the thermal thresholds in both sexes. The response latency decreased equally in both sexes at the 5^{th} and 7^{th} post inoculation day and began to subside by the 10^{th} post inoculation day (Figure 1 A). Mixed-effects ANOVA revealed significant difference for CFA factor, $F_{114} = 81.3$, $P < 0.001$, Time factor, $F_{114} = 14.6$, $P < 0.001$ and interaction CFA X Time, $F_{114} = 8.6$, $P < 0.001$ but was not significant for Sex factor, Sex X Time and Sex X CFA and Sex X Time X CFA (Figure 1 A). Our female data is congruent with the published pain literature underlining the fact that the use of females does not produce substantially larger variance because testing randomly cycling animals negates any cycle confounds (45).

While the deleterious effects of various pain models on the behavior of laboratory rodents is well described, a very few studies make parallel comparison of male and female behavior under pain. Here, we compared the behavior of male and female mice injected with CFA. The mice were tested between the 6 and 10 post inoculation day for anxiety-like behavior, spatial memory, recognition memory and problem-solving ability in this specific order. The CFA injection reduced the percent of time spent in the open arms of the O-maze in males but not in females, Two-way ANOVA showed significant difference for interaction Sex versus CFA ($F_{71} = 7.1$, $P < 0.01$) and CFA factor ($F_{71} = 6.2$, $P < 0.05$) but not for Sex as a factor ($F_{71} = 1.9$, $P > 0.05$) (Figure 1 B).

The Y-maze spontaneous alternation test measures the propensity of rodents to explore new environments over the course of this test; the animals show a tendency to enter a less recently visited arm. Analysis of the test video records demonstrated that male mice subjected to CFA injection made fewer correct alternations when compared to the control males and females of both groups, ANOVA, significant for interaction CFA X Sex, $F_{113} = 6.5$, $P < 0.05$ and CFA factor $F_{113} = 14.4$, $P < 0.001$ but not Sex factor, $F_{113} = 1.6$, $P > 0.05$ (Figure 1 C).

The NOR test is based on the spontaneous tendency of all mammals to investigate novelties in their environment. The injection of CFA decreased the time spent with the novel object in male mice but not in female mice, ANOVA significant difference for Sex, $F_{94} = 5.4$, $P < 0.05$, CFA, $F_{94} = 8.7$, $P<0.001$ and interaction Sex X CFA, $F_{94} = 6.3$, $P < 0.05$, (Figure 1 D).

The puzzle test relies on the natural rodent avoidance of bright open spaces and it measures the time that it takes for the mouse in a bright-lit compartment to remove an obstacle and enter the dark compartment. Here again, only the performance of males was affected by the CFA injection as seen by their increased latency to enter the dark compartment but the CFA injection did not affect the latency to remove the obstacle in females, ANOVA, significant difference for CFA factor, $F_{101} = 11$, $P < 0.001$, significant difference for Sex factor, $F_{101} = 5$, $P < 0.05$ and significant for interaction of Sex X CFA, $F_{101} = 5$, $P < 0.05$ (Figure 1 E).

Altogether, the results of our first experiments showed that while both sexes developed hyperesthesia with the same severity, only male behavior is affected by the inflammatory pain.

Inflammatory pain increases neuronal activity in the mPFC of male but not female mice.

The outcomes of the behavior experiments described above led us to hypothesize that the CFA injection would have different effects on the mPFC activity in males or females. We investigated the neural activity of the mPFC by wireless fiber photometry, which allows for detection of changes in the fluorescent signal generated by Ca^{2+} biosensor. Fiber optic cannulae were implanted into the right mPFC three weeks after stereotaxic injections of pENN-AAV_5-CamKII-GCaMP6f in mice of both sexes. The GCaMP6f fluorescent signal was recorded from freely moving mice for five minutes after placing them on elevated O-maze. The photometric recordings were repeated again eight days after CFA injection and the intensity of the fluorescent signal before and after CFA injections was compared for each mouse. The amplitude of the Ca^{2+} fluorescence, an indicator for neuronal activity, increased

significantly only in male mice with pain, while the signal remained unchanged in females subjected to inflammatory pain; males, paired T-test, $t_8 = 2.4$, $P < 0.05$, females $t_5 = 0.9$, $P > 0.05$, (Figure 2).

Inflammatory pain increases c-Fos immunoreactivity in the LC of males.

If sex differences observed in the behavior tests of mice with pain stem from sex difference in the LC activity, then the expression of markers for neuronal activation should differ in the LC of males versus females. We compared c-Fos immunoreactivity (as a marker for neuronal activation) after CFA application in LC of male and female mice on the eleventh post inoculation day. Only male mice with CFA injections showed a higher number of c-Fos expressing neurons in the LC when compared to the male controls or to the female groups, ANOVA, significant difference for CFA factor, $F_{26} = 5.4$, $P < 0.05$, significant difference for Sex factor, $F_{26} = 5.6$, $P < 0.05$ and significant difference for interaction of Sex X CFA, $F_{26} = 5.1$, $P < 0.05$, (Figure 3).

Inhibition of mPFC neural projections to LC improves the object recognition memory in male mice but negatively affects the spatial memory of female mice subjected to pain.

Based on the results of the last two experiments we speculated that the hyperactivity of mPFC efferents increases the activity of LC, which would increase anxiety and impair memory in male mice subjected to pain, and that the differences in the LC response to the mPFC input establishes the pain-induced behavioral differences between the sexes. Therefore, we tested if the chemogenetic inhibition of the mPFC to LC projections would affect the cognitive performance of mice injected with CFA. First, as a proof of principle, we verified that the projections from the mPFC to LC are present in outbred CD1 mice, which is a strain of mice not frequently used in pain research. The mice received the anterograde tracer pAAV-CamKII-ArchT-GFP into the mPFC and the expression of the efferent fibers in the pontine region was verified (Figure 4 A). Next, we injected the retrograde tracer rAAV-GAG-eGFP-F2A-cre into the LC which labeled the cell bodies of the projection neurons in the mPFC (Figure 4 B). Finally, we proceeded with bilateral injections of the retrograde rAAV-GAG-eGFP-F2A-cre virus into the LC and the cre-activated AAV-hSyn-DIO-hM4D(Gi)-mChrerry (inhibitory DREADD) into mPFC. As a result, the neurons projecting from mPFC to LC were transduced with inhibitory DREADD-Gi virus. Figure 4 C shows the colocalization of the two viruses in the main projection layer (V) of the mPFC.

Three weeks after the viral injections, all mice received 20 μl of CFA into their left hind paw. The same behavioral tests at the same time intervals as described in our first experiment were conducted after intraperitoneal injection of CNO or saline as a control. The CNO treatment did not alter the thermal hypersensitivity of the mice, in other words, the CNO treatment did not induce analgesia in either sex, ANOVA for CNO, Sex and Interaction, $P > 0.05$ for all.

However, the CNO treatment produced somewhat different behavior outcomes in male and female mice. First, the inhibition of the mPFC projections to LC caused anxiolysis in male and female mice, ANOVA, significant for Treatment, $F_{76} = 9.1$, $P < 0.01$ but not for Sex, $F_{76} = 0.8$, $P > 0.05$ or Interaction, $F_{76} = 0.3$, $P > 0.05$, Figure 5 A. Next, the Y-maze test showed

that while the CNO treatment did not change the percent of correct spontaneous alternations in males, the CNO injection substantially reduced the correct alternations in females, ANOVA, significant for Interaction, $F_{50} = 5.5$, $P < 0.05$ and Treatment, $F_{50} = 8.7$, $P > 0.01$ but not for Sex factor, $F_{50} = 4$, $P = 0.051$, Figure 5 B. In NOR, the chemogenetic inhibition of the mPFC to LC projections greatly increased the preference for the novel object in male mice. However, the inhibition of the mPFC-LC projections did not change the preference for the novel object in females, ANOVA, significant for Interaction, $F_{76} = 9.4$, $P < 0.01$ and Treatment, $F_{76} = 6$, $P < 0.05$ but not for Sex factor, $F_{76} = 0.1$, $P > 0.05$, Figure 5 C. The Puzzle test, which assesses the general cognitive ability of mice, was conducted at day10 post-CFA inoculation. Here, the CNO treatment reduced the latency to remove the tunnel obstacle in male mice but increased the latency to remove the obstacle in female mice, ANOVA, significant for Interaction, $F_{70} = 5.7$, $P < 0.05$, but not significant for Sex, $F_{70} = 0.001$, $P > 0.05$ and Treatment, $F_{70} = 0.3$, $P > 0.05$, Figure 5 D.

Lastly, we assessed the expression of c-Fos in the LC after inhibition of the mPFC to LC projections in mice with inflammatory pain. The mice were euthanized one hour after an O-Maze test. The inhibition of the mPFC to LC pathway changed the c-Fos expression in both sexes. While the males with CNO treatment showed a decrease of c-Fos labeled cells, the females with CNO surprisingly increased the c-Fos expression in LC, ANOVA, significant for Interaction, $F_{27} = 33$, $P < 0.001$, but not significant for Sex, $F_{27} = 2.7$, $P > 0.05$ and Treatment, $F_{27} = 0.2$, $P > 0.05$ (Figure 5 E).

In sum, the chemogenetic inhibition of the mPFC projections to the LC improved object recognition memory in male mice but reduced spatial memory in female mice. The activity of LC, as detected by c-Fos expression, was also altered in opposite ways, it decreased in males but increased in females.

Sex differences in the reciprocal mPFC – LC circuit

Published anatomical data describe two main modes of afferent input to the nucleus, a direct contact with the noradrenergic cells (46) or contact with the surrounding interneurons (47). The interneurons in the dendritic zone of the LC play a role of modulatory interface between the efferent fibers and the nucleus (47). We investigated the innervation of LC and periceruleus neurons by mPFC projections by a method for anterograde transsynaptic tagging of cells, which allows for an input specific anterograde trans-synaptic spread of cre-recombinase (36, 37). The cre-carrier AAV_1-pENN-hSyn-Cre-WPRE-hGH was injected unilaterally into the mPFC and a reporter virus, pAAV-Ef1a-DO-DIO-TdTom-EGFP-WPRE-pA was injected into the LC area on the same side as the cre virus. The reporter virus possesses a cre-dependent switch, which changes the expression of the default tdTomato (red) color to EGFP (green) color (38). The tracing experiment confirmed the dual nature of mPFC efferents with ample postsynaptic cre transfer to LC neurons as well as postsynaptic cre transfer to the interneurons in the surrounding periceruleus area (Figure 6). While a similar number of neurons were found to express EGFP in male and female mice, T-test, $t_{11} = 0.7$, $P > 0.05$, the innervation pattern was different between the sexes. Overall, a higher number of EGFP labeled noradrenergic cells were counted in males than in females, T-test, $t_{11} = 2.3$. $P < 0.05$ (Figure 7). The difference in cell count per bregma level between male

and female mice reached statistical significance at the most caudal extension of the nucleus, T-test, $t_{11} = 3.1$. $P < 0.01$ (Figure 7 E). However, a higher number of EGFP labeled interneurons was observed in females when compared to EGFP labeled interneurons found in males, T-test, $t_{11} = 5$, $P < 0.001$. The interneuron cell count between the sexes was significantly different at two bregma levels, bregma level – 5.3 mm, T-test, $t_{11} = 4.8$, $P < 0.001$ and bregma level – 5.6 mm, T-test, $t_{11} = 2.7$, $P < 0.05$ (Figure 7 F).

Next, we analyzed the pattern of expression of retrogradely labeled LC neurons after injection of the retrograde pENN-AAV-hSyn-HI-eGFP-Cre-WPRE-SV40 virus into the mPFC. The noradrenergic cells of LC were visualized by immunostaining for TH. The retrogradely labeled cells expressing the viral GFP were found grouped in the dorsal region of the nucleus throughout the rostro-caudal extent of the structure (Figure 8). The total number of projection neurons from LC to mPFC were higher in female mice (T-test, $t_{13} = 3.6$, $P < 0.01$) with a significant difference at two bregma levels; bregma level – 5.3 mm, T-test, $t_{13} = 3.7$, $P < 0.01$ and bregma level – 5.4 mm, T-test, $t_{13} = 3$, $P < 0.01$ (Figure 8 G).

Discussion

We investigated the effects of inflammatory pain on the activity of the mPFC and LC and compared the cognitive performance of male and female mice. The injection of the inflammatory agent CFA increased the neuronal activity in the mPFC and LC and impaired the cognitive performance of male but not female mice. The chemogenetic inhibition of the mPFC projections to LC improved the object recognition results of the male mice but caused anxiolysis and negatively affected the spatial memory in female mice. Next, we quantified the projection neurons that form up the reciprocal innervation between the mPFC and the LC. While the male LC neurons received more pronounced direct innervation from the mPFC, a higher number of mPFC efferents were found to connect with the periceruleus interneurons in females. And vice versa, the female mice showed a higher number of projection neurons from LC to the mPFC when compared to their male counterparts. In sum, our research relies sex differences in the cognitive impact of inflammatory pain to differences in the wiring pattern between mPFC and LC.

The LC is an integral part of the descending pain inhibitory system and the release of NE in the dorsal horn of the spinal cord causes robust α_2 receptor mediated analgesia (30, 48). We have previously reported a decrease of c-Fos and TH protein expression in the LC of male mice with neuropathic injury (19, 49). Here, we observed quite the opposite, an increase of c-Fos expression in the LC neurons of males injected with CFA. The explanation of this phenomenon rests in the duration of nociceptive stimulus; while acute inflammatory pain activates LC neurons (17), long-lasting neuropathic pain tends to reduce the activity of the nucleus (18, 50). This bimodal pattern of LC activity is described as the very likely mechanisms for pain chronification in which overactivation of LC by recent pain is followed by deactivation of the nucleus overtime with an end result suppression of NE release in the spinal cord and decrease of NE mediated analgesia (32). The high c-Fos expression in the LC of male mice with CFA indicates that the relatively short-lasting inflammatory pain model used in our study does not lead to pain chronification.

Various pain models link the overactivity of LC with dysfunction of the mPFC. Published reports show that CFA induced inflammation leads to sprouting of NE fibers into the mPFC (34) and that CFA increases the excitability of mPFC projection neurons (31). Other studies find that neuropathic pain increased the release of NE (33) into the mPFC where NE drives persistent neuronal activity via $alpha_1$ and $alpha_2$ adrenoreceptors (51). All of these studies used male rodents as subjects and their results complement very well our results from the male groups, where the seemingly simultaneous overactivation of the mPFC and LC by inflammatory pain negatively impacted cognitive performance of male mice. By adding females, our study shows that the female anxiety-like behavior and cognitive performance are not affected by the CFA and that the sexual dimorphism of the neuronal wiring between mPFC and LC very likely renders females resilient to the effects of inflammatory pain.

Interestingly, other anatomical and functional sex differences in the neuronal circuits engaged in various facets of the pain experience have already been described. The sexually dimorphic response to the actions of morphine in the CFA pain model is attributed to the anatomical differences of the pathway linking the vlPAG to the rostral ventrolateral medulla (52); the sex differences in the hypothalamic projections to LC result in different responses to thermal pain after inhibition of LC (53). As mentioned above, the well described descending pain modulatory system encompasses LC (5), a nucleus with confirmed sexual dimorphism. The female LC is larger because it contains a greater number of neurons (54) with more complex dendritic arborization (55, 56). The anatomical differences between male and female LC are based on gene expression and molecular differences (57), which result in sustained resistance of the female LC to desensitization by stressors (21). Our investigation adds one more element to the already established sex differences in the LC anatomy. While the total number of neurons in the LC area receiving direct innervation from the mPFC was similar between the sexes (56 cells in females versus 49 cells in males), in females, the postsynaptic cre transfer affected a higher number of periceruleus interneurons than the neurons of LC proper. Based on the published electrophysiological studies about the dual nature of the mPFC to LC projection being both excitatory and inhibitory (27, 28), we may speculate that the male LC receives a heightened excitatory input from the mPFC, while the activation of the female LC by the mPFC projections may be balanced by stronger inhibition via the surrounding pool of interneurons. The number of projecting neurons was reversed in the LC to mPFC direction, where the average was higher in females than in males (69 cells versus 35 cells). This observation is akin to the current view about sex differences in NE signaling which links the high levels of arousal and hypervigilance to the higher levels of NE in the CNS of females (58).

A limitation of our study is the lack of information about the brain regions where the top-down regulation of the mPFC modulates NE release. An adequate answer would require measuring of NE release in an array of brain regions that receive innervation from LC and participate in various aspects of cognitive processes. This is a formidable task, which likely will be included as a long-term project of our lab but it is beyond the scope of the current study. Additional complexity lays in the functional organization of the LC. It is accepted that LC consists of discrete subdivisions, these subdivisions can be activated independently of each other and execute different, even opposing functions in specific brain regions (59). An example of this heterogeneous activity is that while fear learning activates LC projections to

the basolateral amygdala, fear extinction activates LC projections to the mPFC (13). The NE signaling receives additional fine-tuning by activation of the excitatory α_1 and β, and inhibitory α_2 adrenergic receptors, all with different affinity for NE and opposing actions on memory and attention (60). The differential affinity of adrenergic receptors for NE results in an inverted U-shaped curve for various physiological responses and explains how either inadequate or excessive NE release negatively affects cognitive and memory processes. While our studies do not directly measure NE release in various regions of the CNS or the activity of specific LC subregions, they clearly establish the sexual dimorphism of the reciprocal wiring between the mPFC and the LC. The cognitive tests included in this project were chosen because the published literature shows evidence for the dependence of these cognitive tasks on the mPFC and that pain negatively impacts most of them (43, 61–65). On the other hand, the involvement the mPFC and more specifically the PrL region in the modulation of the affective and sensory components of pain is well established (2, 66, 67). There is also compelling evidence that pain increases the NE signaling into the mPFC (33, 34) and causes loss of attention and memory impairment by overactivation of the noradrenergic α_1 receptors (60). Interestingly, a chronic stress study links the deleterious cognitive effects of chronic unpredictable stress to the increased NE release in the cortex (68). The study also demonstrates that the cognitive deficits can be prevented by blocking NE transmission in the mPFC (68). This finding is somewhat similar to our observation that the inhibition of mPFC to LC pathway improves the long-term memory of male mice with overactive LC. All these facts make very plausible the idea that the changes in the NE transmission in the mPFC is responsible for the observed behavior outcomes. Overall, our most concise interpretation of the observed behavior results is that the inflammatory pain creates a positive feedback between the mPFC and the LC, where an overactive mPFC maintains the activity of LC and increases NE release in the mPFC, which leads to anxiety and cognitive impairment in male mice. In female mice, the input from the mPFC to the LC targets a greater number of inhibitory interneurons in the periceruleus area and this innervation pattern abates the overactivation of LC by the mPFC. However, as we pointed out, a more comprehensive investigation of the mPFC regulation of NE release into various limbic structures such as the mPFC, amygdala, hippocampus and hypothalamus is needed in order to provide a full description of the modulatory regulation of the LC by the mPFC efferents.

In sum, our research casts light on important anatomical and functional pathway and certain sex differences in the regulation of LC by the mPFC, which besides its functional implications may also be a background for various pathologies linked to NE signaling, such as affective disorders, cognitive impairment and chronification of pain.

List of Abbreviations:

AAV	adeno-associated virus
CFA	complete Freund’s adjuvant
Cg	cingulate cortex
CNO	Clozapine N-Oxide

CNS	central nervous system
DP	dorsal peduncular cortex
DREADD	designer receptors exclusively activated by designer drug
EGFP	enhanced green fluorescent protein
fmi	forceps minor of the corpus callosum
GFP	green fluorescent protein
IL	infralimbic cortex
LC	locus ceruleus
mPFC	medial prefrontal cortex
NET	norepinephrine transporter
NE	norepinephrine
NOR	novel object recognition test
PBS	phosphate buffered saline
PrL	prelimbic cortex
TH	tyrosine hydroxylase
vlPAG	ventrolateral periaqueductal gray

References

1. Usdin TB, and Dimitrov EL (2016) The Effects of Extended Pain on Behavior: Recent Progress. *Neuroscientist* 22, 521–533 [PubMed: 27621368]
2. Kummer KK, Mitric M, Kalpachidou T, and Kress M (2020) The Medial Prefrontal Cortex as a Central Hub for Mental Comorbidities Associated with Chronic Pain. Int J Mol Sci 21
3. Alba-Delgado C, Llorca-Torralba M, Horrillo I, Ortega JE, Mico JA, Sanchez-Blazquez P, Meana JJ, and Berrocoso E (2013) Chronic pain leads to concomitant noradrenergic impairment and mood disorders. Biol Psychiatry 73, 54–62 [PubMed: 22854119]
4. Drake RA, Steel KA, Apps R, Lumb BM, and Pickering AE (2021) Loss of cortical control over the descending pain modulatory system determines the development of the neuropathic pain state in rats. Elife 10
5. Ossipov MH, Morimura K, and Porreca F (2014) Descending pain modulation and chronification of pain. Curr Opin Support Palliat Care 8, 143–151 [PubMed: 24752199]
6. Clewett DV, Huang R, Velasco R, Lee TH, and Mather M (2018) Locus Coeruleus Activity Strengthens Prioritized Memories Under Arousal. J Neurosci 38, 1558–1574 [PubMed: 29301874]
7. Sales AC, Friston KJ, Jones MW, Pickering AE, and Moran RJ (2019) Locus Coeruleus tracking of prediction errors optimises cognitive flexibility: An Active Inference model. PLoS Comput Biol 15, e1006267 [PubMed: 30608922]
8. Franowicz JS, Kessler LE, Borja CM, Kobilka BK, Limbird LE, and Arnsten AF (2002) Mutation of the alpha2A-adrenoceptor impairs working memory performance and annuls cognitive enhancement by guanfacine. J Neurosci 22, 8771–8777 [PubMed: 12351753]

9. Radley JJ, Williams B, and Sawchenko PE (2008) Noradrenergic innervation of the dorsal medial prefrontal cortex modulates hypothalamo-pituitary-adrenal responses to acute emotional stress. J Neurosci 28, 5806–5816 [PubMed: 18509042]
10. Morilak DA, Barrera G, Echevarria DJ, Garcia AS, Hernandez A, Ma S, and Petre CO (2005) Role of brain norepinephrine in the behavioral response to stress. Prog Neuropsychopharmacol Biol Psychiatry 29, 1214–1224 [PubMed: 16226365]
11. Llorca-Torralba M, Borges G, Neto F, Mico JA, and Berrocoso E (2016) Noradrenergic Locus Coeruleus pathways in pain modulation. Neuroscience 338, 93–113 [PubMed: 27267247]
12. Howorth PW, Teschemacher AG, and Pickering AE (2009) Retrograde adenoviral vector targeting of nociresponsive pontospinal noradrenergic neurons in the rat in vivo. J Comp Neurol 512, 141–157 [PubMed: 19003793]
13. Uematsu A, Tan BZ, Ycu EA, Cuevas JS, Koivumaa J, Junyent F, Kremer EJ, Witten IB, Deisseroth K, and Johansen JP (2017) Modular organization of the brainstem noradrenaline system coordinates opposing learning states. Nat Neurosci 20, 1602–1611 [PubMed: 28920933]
14. Chandler DJ, Gao WJ, and Waterhouse BD (2014) Heterogeneous organization of the locus coeruleus projections to prefrontal and motor cortices. Proc Natl Acad Sci U S A 111, 6816–6821 [PubMed: 24753596]
15. Uematsu A, Tan BZ, and Johansen JP (2015) Projection specificity in heterogeneous locus coeruleus cell populations: implications for learning and memory. Learn Mem 22, 444–451 [PubMed: 26330494]
16. Hickey L, Li Y, Fyson SJ, Watson TC, Perrins R, Hewinson J, Teschemacher AG, Furue H, Lumb BM, and Pickering AE (2014) Optoactivation of locus ceruleus neurons evokes bidirectional changes in thermal nociception in rats. J Neurosci 34, 4148–4160 [PubMed: 24647936]
17. Moriya S, Yamashita A, Nishi R, Ikoma Y, Yamanaka A, and Kuwaki T (2019) Acute nociceptive stimuli rapidly induce the activity of serotonin and noradrenalin neurons in the brain stem of awake mice. IBRO Rep 7, 1–9 [PubMed: 31194165]
18. Hayashida KI, and Eisenach JC (2018) Descending Noradrenergic Inhibition: An Important Mechanism of Gabapentin Analgesia in Neuropathic Pain. Adv Exp Med Biol 1099, 93–100 [PubMed: 30306517]
19. Andreoli M, Marketkar T, and Dimitrov E (2017) Contribution of amygdala CRF neurons to chronic pain. Exp Neurol 298, 1–12 [PubMed: 28830762]
20. Hughes SW, Hickey L, Hulse RP, Lumb BM, and Pickering AE (2013) Endogenous analgesic action of the pontospinal noradrenergic system spatially restricts and temporally delays the progression of neuropathic pain following tibial nerve injury. Pain 154, 1680–1690 [PubMed: 23707289]
21. Bangasser DA, Wiersielis KR, and Khantsis S (2016) Sex differences in the locus coeruleus-norepinephrine system and its regulation by stress. Brain Res 1641, 177–188 [PubMed: 26607253]
22. Kim M-A, and Lee HS (2003) Descending projections from the prefrontal cortex to the locus ceruleus of the rat. Korean J Bio Sci 7, 49–55
23. Euston DR, Gruber AJ, and McNaughton BL (2012) The role of medial prefrontal cortex in memory and decision making. Neuron 76, 1057–1070 [PubMed: 23259943]
24. Van Eden CG, and Buijs RM (2000) Functional neuroanatomy of the prefrontal cortex: autonomic interactions. Prog Brain Res 126, 49–62 [PubMed: 11105639]
25. McKlveen JM, Myers B, and Herman JP (2015) The medial prefrontal cortex: coordinator of autonomic, neuroendocrine and behavioural responses to stress. J Neuroendocrinol 27, 446–456 [PubMed: 25737097]
26. Ong WY, Stohler CS, and Herr DR (2019) Role of the Prefrontal Cortex in Pain Processing. Mol Neurobiol 56, 1137–1166 [PubMed: 29876878]
27. Jodo E, Chiang C, and Aston-Jones G (1998) Potent excitatory influence of prefrontal cortex activity on noradrenergic locus coeruleus neurons. Neuroscience 83, 63–79 [PubMed: 9466399]
28. Sara SJ, and Herve-Minvielle A (1995) Inhibitory influence of frontal cortex on locus coeruleus neurons. Proc Natl Acad Sci U S A 92, 6032–6036 [PubMed: 7597075]

29. Joshi S, Li Y, Kalwani RM, and Gold JI (2016) Relationships between Pupil Diameter and Neuronal Activity in the Locus Coeruleus, Colliculi, and Cingulate Cortex. Neuron 89, 221–234 [PubMed: 26711118]
30. Huang J, Gadotti VM, Chen L, Souza IA, Huang S, Wang D, Ramakrishnan C, Deisseroth K, Zhang Z, and Zamponi GW (2019) A neuronal circuit for activating descending modulation of neuropathic pain. Nat Neurosci 22, 1659–1668 [PubMed: 31501573]
31. Wu XB, Liang B, and Gao YJ (2016) The increase of intrinsic excitability of layer V pyramidal cells in the prelimbic medial prefrontal cortex of adult mice after peripheral inflammation. Neurosci Lett 611, 40–45 [PubMed: 26592167]
32. Parent AJ, Tetreault P, Roux M, Belleville K, Longpre JM, Beaudet N, Goffaux P, and Sarret P (2016) Descending nociceptive inhibition is modulated in a time-dependent manner in a double-hit model of chronic/tonic pain. Neuroscience 315, 70–78 [PubMed: 26691963]
33. Suto T, Eisenach JC, and Hayashida K (2014) Peripheral nerve injury and gabapentin, but not their combination, impair attentional behavior via direct effects on noradrenergic signaling in the brain. Pain 155, 1935–1942 [PubMed: 24837843]
34. Cordeiro Matos S, Zamfir M, Longo G, Ribeiro-da-Silva A, and Seguela P (2018) Noradrenergic fiber sprouting and altered transduction in neuropathic prefrontal cortex. Brain Struct Funct 223, 1149–1164 [PubMed: 29094305]
35. Tuttle AH, Philip VM, Chesler EJ, and Mogil JS (2018) Comparing phenotypic variation between inbred and outbred mice. Nat Methods 15, 994–996 [PubMed: 30504873]
36. Zingg B, Chou XL, Zhang ZG, Mesik L, Liang F, Tao HW, and Zhang LI (2017) AAV-Mediated Anterograde Transsynaptic Tagging: Mapping Corticocollicular Input-Defined Neural Pathways for Defense Behaviors. Neuron 93, 33–47 [PubMed: 27989459]
37. Zingg B, Peng B, Huang J, Tao HW, and Zhang LI (2020) Synaptic Specificity and Application of Anterograde Transsynaptic AAV for Probing Neural Circuitry. J Neurosci 40, 3250–3267 [PubMed: 32198185]
38. Saunders A, and Sabatini BL (2015) Cre Activated and Inactivated Recombinant Adeno-Associated Viral Vectors for Neuronal Anatomical Tracing or Activity Manipulation. Curr Protoc Neurosci 72, 1 24 21–21 24 15 [PubMed: 26131660]
39. Fehrenbacher JC, Vasko MR, and Duarte DB (2012) Models of inflammation: Carrageenan- or complete Freund's Adjuvant (CFA)-induced edema and hypersensitivity in the rat. Curr Protoc Pharmacol Chapter 5, Unit5 4
40. Gunaydin LA, Grosenick L, Finkelstein JC, Kauvar IV, Fenno LE, Adhikari A, Lammel S, Mirzabekov JJ, Airan RD, Zalocusky KA, Tye KM, Anikeeva P, Malenka RC, and Deisseroth K (2014) Natural neural projection dynamics underlying social behavior. Cell 157, 1535–1551 [PubMed: 24949967]
41. Ohtani S, Fujita S, Hasegawa K, Tsuda H, Tonogi M, and Kobayashi M (2018) Relationship between the fluorescence intensity of rhodamine-labeled orexin A and the calcium responses in cortical neurons: An in vivo two-photon calcium imaging study. J Pharmacol Sci 138, 76–82 [PubMed: 30293961]
42. Shepard R, Beckett E, and Coutellier L (2017) Assessment of the acquisition of executive function during the transition from adolescence to adulthood in male and female mice. Dev Cogn Neurosci 28, 29–40 [PubMed: 29102727]
43. Ben Abdallah NM, Fuss J, Trusel M, Galsworthy MJ, Bobsin K, Colacicco G, Deacon RM, Riva MA, Kellendonk C, Sprengel R, Lipp HP, and Gass P (2011) The puzzle box as a simple and efficient behavioral test for exploring impairments of general cognition and executive functions in mouse models of schizophrenia. Exp Neurol 227, 42–52 [PubMed: 20851119]
44. Guettier JM, Gautam D, Scarselli M, Ruiz de Azua I, Li JH, Rosemond E, Ma X, Gonzalez FJ, Armbruster BN, Lu H, Roth BL, and Wess J (2009) A chemical-genetic approach to study G protein regulation of beta cell function in vivo. Proc Natl Acad Sci U S A 106, 19197–19202 [PubMed: 19858481]
45. Mogil JS, and Chanda ML (2005) The case for the inclusion of female subjects in basic science studies of pain. Pain 117, 1–5 [PubMed: 16098670]

46. Reyes BA, Bangasser DA, Valentino RJ, and Van Bockstaele EJ (2014) Using high resolution imaging to determine trafficking of corticotropin-releasing factor receptors in noradrenergic neurons of the rat locus coeruleus. Life Sci 112, 2–9 [PubMed: 25058917]
47. Aston-Jones G, Zhu Y, and Card JP (2004) Numerous GABAergic afferents to locus ceruleus in the pericerulear dendritic zone: possible interneuronal pool. J Neurosci 24, 2313–2321 [PubMed: 14999082]
48. Stone LS, MacMillan LB, Kitto KF, Limbird LE, and Wilcox GL (1997) The alpha2a adrenergic receptor subtype mediates spinal analgesia evoked by alpha2 agonists and is necessary for spinal adrenergic-opioid synergy. J Neurosci 17, 7157–7165 [PubMed: 9278550]
49. Cardenas A, Caniglia J, Keljalic D, and Dimitrov E (2020) Sex differences in the development of anxiodepressive-like behavior of mice subjected to sciatic nerve cuffing. Pain 161, 1861–1871 [PubMed: 32701845]
50. Hayashida KI, and Obata H (2019) Strategies to Treat Chronic Pain and Strengthen Impaired Descending Noradrenergic Inhibitory System. Int J Mol Sci 20
51. Zhang Z, Cordeiro Matos S, Jego S, Adamantidis A, and Seguela P (2013) Norepinephrine drives persistent activity in prefrontal cortex via synergistic alpha1 and alpha2 adrenoceptors. PLoS One 8, e66122 [PubMed: 23785477]
52. Loyd DR, and Murphy AZ (2006) Sex differences in the anatomical and functional organization of the periaqueductal gray-rostral ventromedial medullary pathway in the rat: a potential circuit mediating the sexually dimorphic actions of morphine. J Comp Neurol 496, 723–738 [PubMed: 16615128]
53. Wagner M, Banerjee T, Jeong Y, and Holden JE (2016) Sex differences in hypothalamic-mediated tonic norepinephrine release for thermal hyperalgesia in rats. Neuroscience 324, 420–429 [PubMed: 27001177]
54. Pinos H, Collado P, Rodriguez-Zafra M, Rodriguez C, Segovia S, and Guillamon A (2001) The development of sex differences in the locus coeruleus of the rat. Brain Res Bull 56, 73–78 [PubMed: 11604252]
55. Bangasser DA, Zhang X, Garachh V, Hanhauser E, and Valentino RJ (2011) Sexual dimorphism in locus coeruleus dendritic morphology: a structural basis for sex differences in emotional arousal. Physiol Behav 103, 342–351 [PubMed: 21362438]
56. Luque JM, de Blas MR, Segovia S, and Guillamon A (1992) Sexual dimorphism of the dopamine-beta-hydroxylase-immunoreactive neurons in the rat locus ceruleus. Brain Res Dev Brain Res 67, 211–215 [PubMed: 1511516]
57. Mulvey B, Bhatti DL, Gyawali S, Lake AM, Kriaucionis S, Ford CP, Bruchas MR, Heintz N, and Dougherty JD (2018) Molecular and Functional Sex Differences of Noradrenergic Neurons in the Mouse Locus Coeruleus. Cell Rep 23, 2225–2235 [PubMed: 29791834]
58. Bangasser DA, Eck SR, and Ordones Sanchez E (2019) Sex differences in stress reactivity in arousal and attention systems. Neuropsychopharmacology 44, 129–139 [PubMed: 30022063]
59. Chandler DJ, Jensen P, McCall JG, Pickering AE, Schwarz LA, and Totah NK (2019) Redefining Noradrenergic Neuromodulation of Behavior: Impacts of a Modular Locus Coeruleus Architecture. J Neurosci 39, 8239–8249 [PubMed: 31619493]
60. Berridge CW, and Spencer RC (2016) Differential cognitive actions of norepinephrine a2 and a1 receptor signaling in the prefrontal cortex. Brain Res 1641, 189–196 [PubMed: 26592951]
61. Cardoso-Cruz H, Paiva P, Monteiro C, and Galhardo V (2019) Selective optogenetic inhibition of medial prefrontal glutamatergic neurons reverses working memory deficits induced by neuropathic pain. Pain 160, 805–823 [PubMed: 30681984]
62. Moriarty O, Gorman CL, McGowan F, Ford GK, Roche M, Thompson K, Dockery P, McGuire BE, and Finn DP (2016) Impaired recognition memory and cognitive flexibility in the rat L5-L6 spinal nerve ligation model of neuropathic pain. Scand J Pain 10, 61–73 [PubMed: 28361775]
63. Cardoso-Cruz H, Lima D, and Galhardo V (2013) Impaired spatial memory performance in a rat model of neuropathic pain is associated with reduced hippocampus-prefrontal cortex connectivity. J Neurosci 33, 2465–2480 [PubMed: 23392675]

64. Shah AA, and Treit D (2003) Excitotoxic lesions of the medial prefrontal cortex attenuate fear responses in the elevated-plus maze, social interaction and shock probe burying tests. Brain Res 969, 183–194 [PubMed: 12676379]

65. Tuscher JJ, Taxier LR, Fortress AM, and Frick KM (2018) Chemogenetic inactivation of the dorsal hippocampus and medial prefrontal cortex, individually and concurrently, impairs object recognition and spatial memory consolidation in female mice. Neurobiol Learn Mem 156, 103–116 [PubMed: 30408525]

66. Wang GQ, Cen C, Li C, Cao S, Wang N, Zhou Z, Liu XM, Xu Y, Tian NX, Zhang Y, Wang J, Wang LP, and Wang Y (2015) Deactivation of excitatory neurons in the prelimbic cortex via Cdk5 promotes pain sensation and anxiety. Nat Commun 6, 7660 [PubMed: 26179626]

67. Fan XC, Fu S, Liu FY, Cui S, Yi M, and Wan Y (2018) Hypersensitivity of Prelimbic Cortex Neurons Contributes to Aggravated Nociceptive Responses in Rats With Experience of Chronic Inflammatory Pain. Front Mol Neurosci 11, 85 [PubMed: 29623029]

68. Jett JD, and Morilak DA (2013) Too much of a good thing: blocking noradrenergic facilitation in medial prefrontal cortex prevents the detrimental effects of chronic stress on cognition. Neuropsychopharmacology 38, 585–595 [PubMed: 23132268]

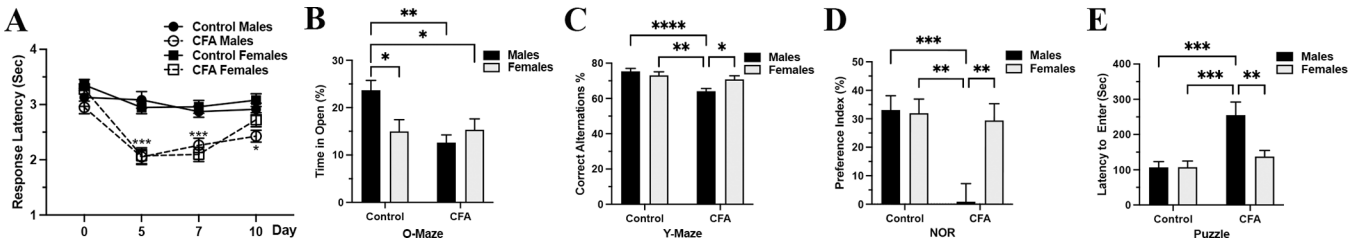

Figure 1: While injection of CFA causes thermal hypersensitivity in both sexes, the anxiety-like behavior, spatial and long-term memory, and puzzle solving abilities are not affected equally in male and female mice.

A) The CFA injection lowered the thermal thresholds in both sexes between 0 day and day 7 - ***, P<0.001 and the effect subsided by day 10 when only the response latency of the CFA male group was still lower than the controls - *, P<0.05. **B)** Only male mice with CFA injection spent less time in the open arms of the elevated O-maze, post-hoc analysis: ** - control males vs. CFA males, P < 0.01; * - control males vs. control females, P < 0.05, and * - control males vs. CFA females, P < 0.05. **C)** Male mice injected with CFA made fewer correct alternations on Y-maze, Post-hoc analysis: *** - control males vs. CFA males, P < 0.001; *- CFA males vs. CFA females, P < 0.05 and ** - control females vs. CFA males, P < 0.01. **D)** NOR also showed differences between male and female mice; while male mice injected with CFA spent less time with the new object, the performance of the female mice was not affected, Post-hoc analysis: *** - control males vs. CFA males, P < 0.001; ** - control females vs. CFA males, P < 0.01 and ** - CFA males vs. CFA females, P < 0.01. **E)** Similarly, inflammatory pain caused by CFA injection increased the latency to enter the dark compartment of the puzzle box only in males, while the female time to enter was not affected at all, Post-hoc analysis: *** - control males vs. CFA males, P < 0.001; *** - control females vs. CFA males, P < 0.001 and ** - CFA males vs. CFA females, P < 0.01. Data expressed as mean ± SEM.

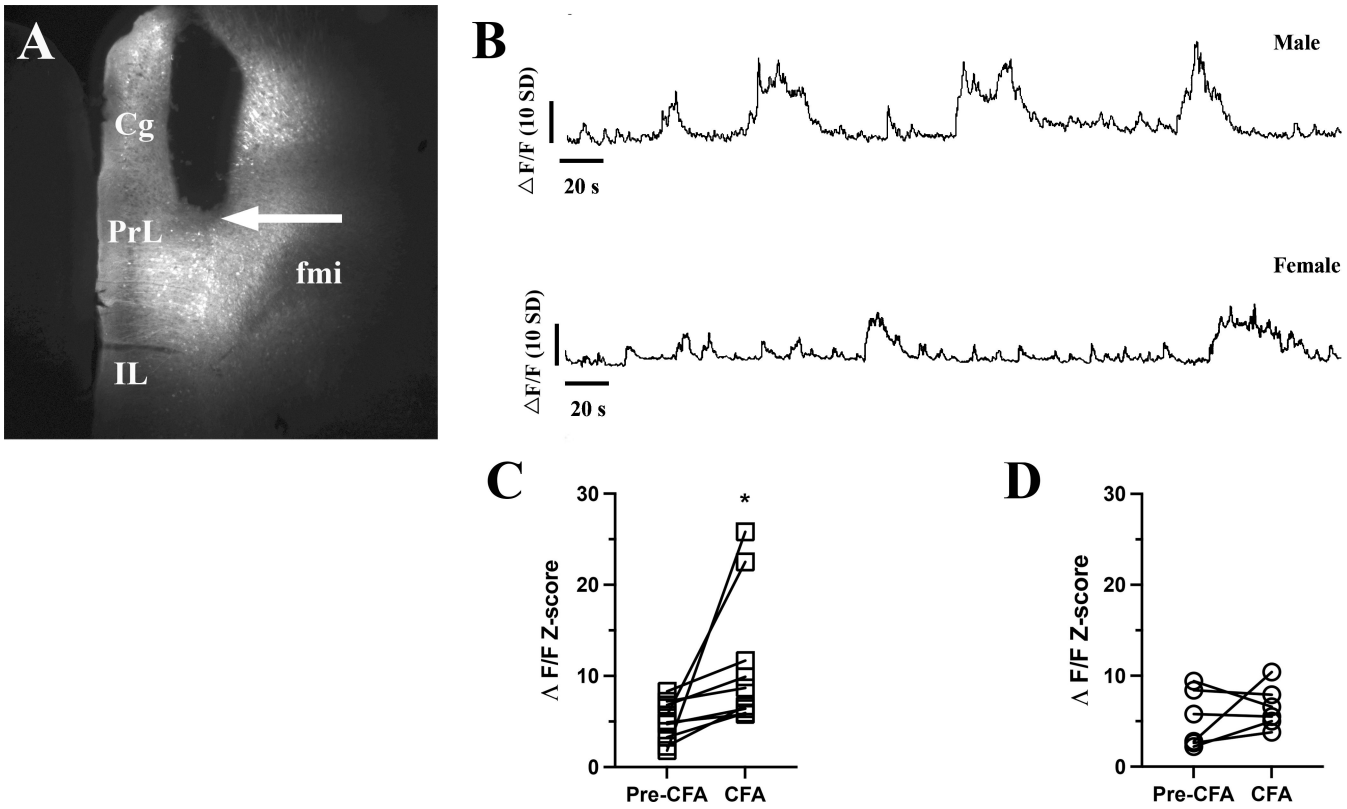

Figure 2: Inflammatory pain increases the neuronal activity of the mPFC neurons in freely moving male mice but not in female mice.

Panel **A** shows the placement of the photometric fiber-optic cannula in the mPFC. The arrow points to the cannula end positioned above the transduced neurons occupying the deep layers of the PrL, a subdivision of mPFC. Panel **B** shows the continuous fiber photometry recordings from a male (upper trace) and female (lower trace) mice. The mice ambulated on elevated O-maze during the recordings, eight days after CFA injection into the hind paw. The graph in panel **C** is the mean z-scored change in fluorescent signal (ΛF/F) of male mice after eight days with inflammatory pain, where the CFA injection caused significant increase of the detected fluorescence triggered by Ca^{2+} transients (Paired T-test, $t_8 = 2.4$, $P < 0.05$). Panel **D** is the mean z-scored change in ΛF/F of female mice with inflammatory pain. The CFA injection did not change the intensity of the fluorescent signal (Paired T-test, $t_5 = 0.9$, $P > 0.05$). Data expressed as individual points. Abbreviations: Cg – cingulate cortex, fmi – forceps minor of the corpus callosum, IL – infralimbic cortex, PrL – prelimbic cortex.

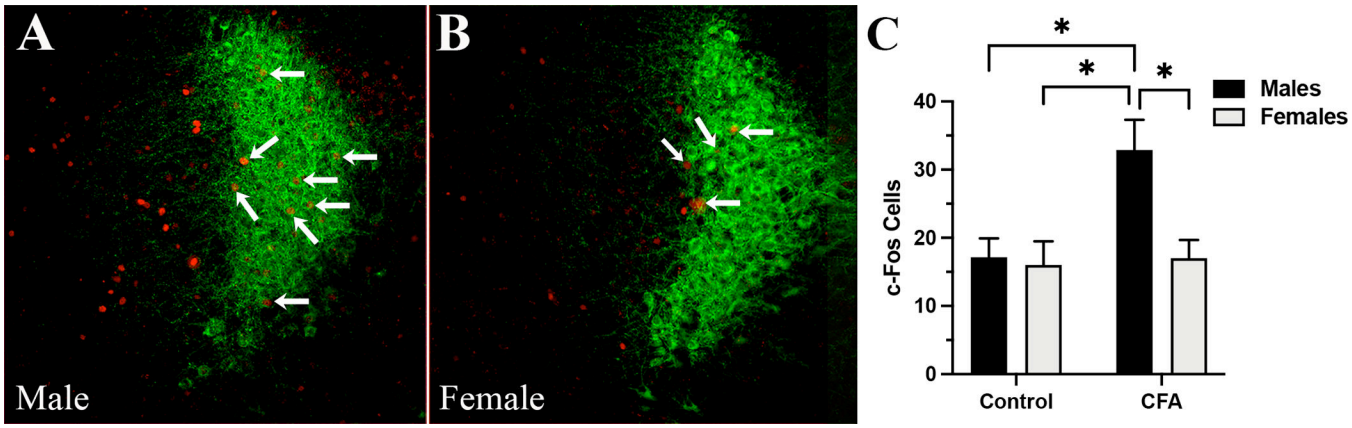

Figure 3: The number of c-Fos expressing cells is higher in the LC of male mice than female mice subjected to inflammatory pain.

Expression of c-Fos (red) in the LC (green, immunostaining for NE-transporter) of **(A)** male and **(B)** female mouse. An average, fewer c-Fos labeled LC neurons were found in females when compared to male mice injected with CFA. **C)** Post-hoc analysis: * - control males vs. CFA males, $P < 0.05$; * - CFA males vs. CFA females, $P < 0.05$ and * - control females vs. CFA males, $P < 0.05$. Data expressed as mean ± SEM.

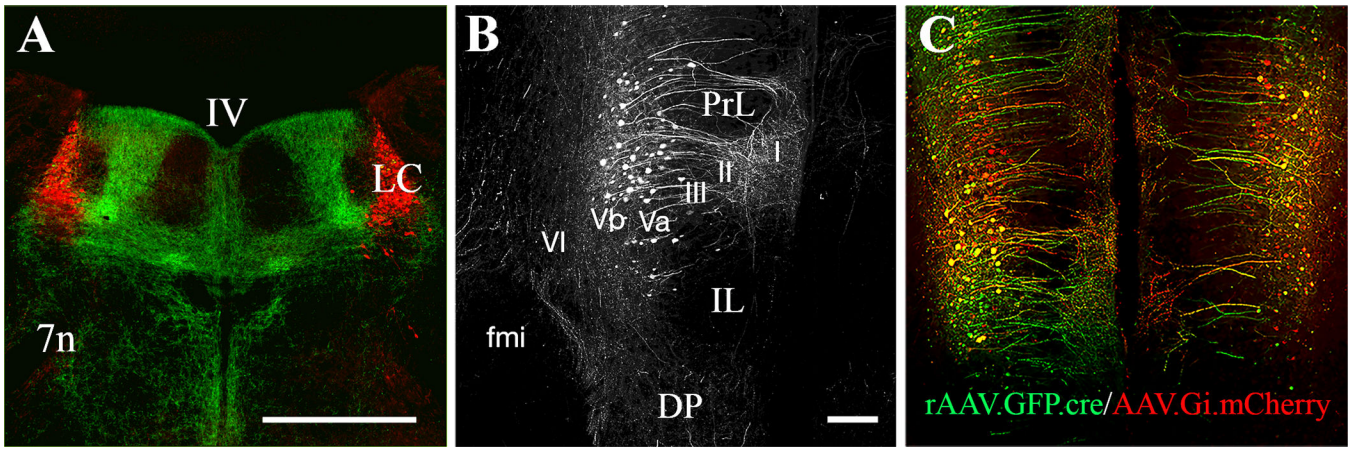

Figure 4. The mPFC sends robust projections to the LC in CD1 mouse strain.

Panel **A** shows the expression of efferent fibers (green) in the pontine area at the level of LC (red), which were labeled after injection of the anterograde tracer AAV_1-CamKII-ArchT-GFP into the mPFC. The cortical efferents target the most dorsal and ventral parts of the medial LC dendritic zone with a relatively sparse expression in the center of the medial and the lateral periceruleus dendritic zones. Panel **B** shows the cell bodies of mPFC neurons labeled after injection of the retrograde rAAV-GAG-eGFP-F2A-cre into the LC. The projection neurons occupy the 5^{th} cortical layer of the PrL, as a subdivision of mPFC, with a very few neuronal bodies localized in the IL. Panel **C** shows the colocalization of the retrograde rAAV-GAG-eGFP-F2A-cre (green) injected into LC and the cre-dependent inhibitory AAV-hSyn-DIO-hM4D(Gi)-mCherry (red) injected into mPFC. These bilateral viral injections allow for chemogenetic inhibition of the mPFC projections to LC. The mice were killed for immunostaining three weeks after the viral injections, which is the time necessary for optimal viral expression. Abbreviations: Roman numerals from I to VI in panel B – cortical layers, IV in panel A – 4th ventricle, 7n – the nucleus of the seventh cranial nerve, DP – dorsal peduncular cortex, fmi – forceps minor of the corpus callosum, IL – infralimbic cortex, LC – locus ceruleus, PrL – prelimbic cortex. Scale bar = 500 μm in A and 100 μm in B and C.

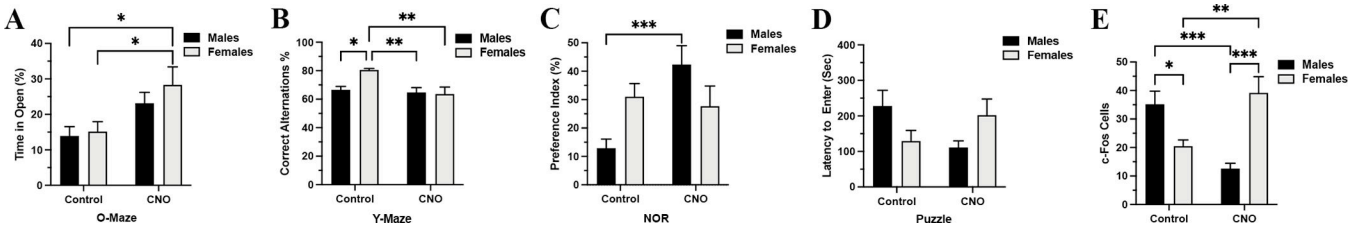

Figure 5: Chemogenetic inhibition of the mPFC projections to the LC affects differently the behavior of male and female mice subjected to inflammatory pain.

A) The CNO treatment increased the time spent in the open quadrants of the O-Maze in female mice, Post-hoc analysis: * - control females vs. CNO females, $P < 0.05$ and * - control males vs. CNO females, $P < 0.05$. **B)** shows the reduced number of correct alternations in female mice after CNO treatment, Post-hoc analysis: ** - control females vs. CFA females, $P < 0.01$; ** - control females vs. CFA males, $P < 0.01$ and * - control males vs. control females, $P < 0.05$. **C)** the panel compares the preference for the novel object after CNO treatment, where males show an increased preference for the novel object but female's preference for the novel object remained unaltered, Post-hoc analysis: * - control males vs. CFA males, $P < 0.05$. **D)** shows the effect of CNO treatment on the puzzle test performance, where the CNO treatment produced a noticeable sex versus CNO interaction but the post-hoc analysis did not detect statistically significant changes in the latency to remove the obstacle in any group. **E)** the panel compares c-Fos expression in the LC after CNO injection between male and female mice, Post-hoc analysis: * - control males vs. control females, $P < 0.05$; *** - control males vs. CFA males, $P < 0.001$; ** - control females vs. CFA females, $P < 0.01$ and *** - CNO males vs. CNO females, $P < 0.001$. Data expressed as mean ± SEM.

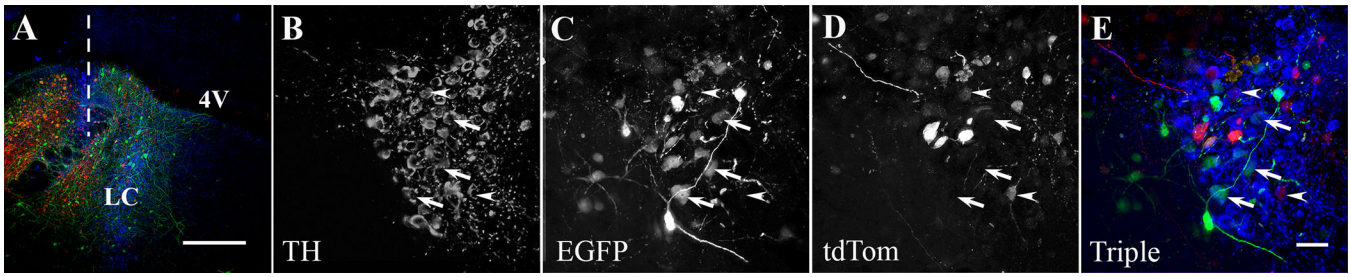

Figure 6: The cre-switch virus pAAV-Ef1a-DO-DIO-TdTom-EGFP labels numerous cells in the rostro lateral pons.

The injection of pAAV-Ef1a-DO-DIO-TdTom-EGFP into the LC region labeled cells in the default red color, but the AAV1-pENN-hSyn-Cre-WPRE-hGH virus injected into the mPFC switched the color to green in cells that directly received cre-recombinase by post-synaptic transfer, an indication for their innervation by the mPFC efferents. **A)** The panel shows the injection tract (interrupted line) and the dispersal of the virus (green and red) in the LC (blue) and the surrounding area. The next three panels show single channel images of TH (B), EGFP (C) and tdTomato (D) labeled neurons. Panel **E** is a composed image of the three channels. The arrows point to TH neurons colocalized with EGFP and the arrowheads to TH neurons colocalized with tdTomato. Abbreviations: 4V - 4th ventricle, LC – locus ceruleus. Scale bar = 400 μm in A and 25 μm in E.

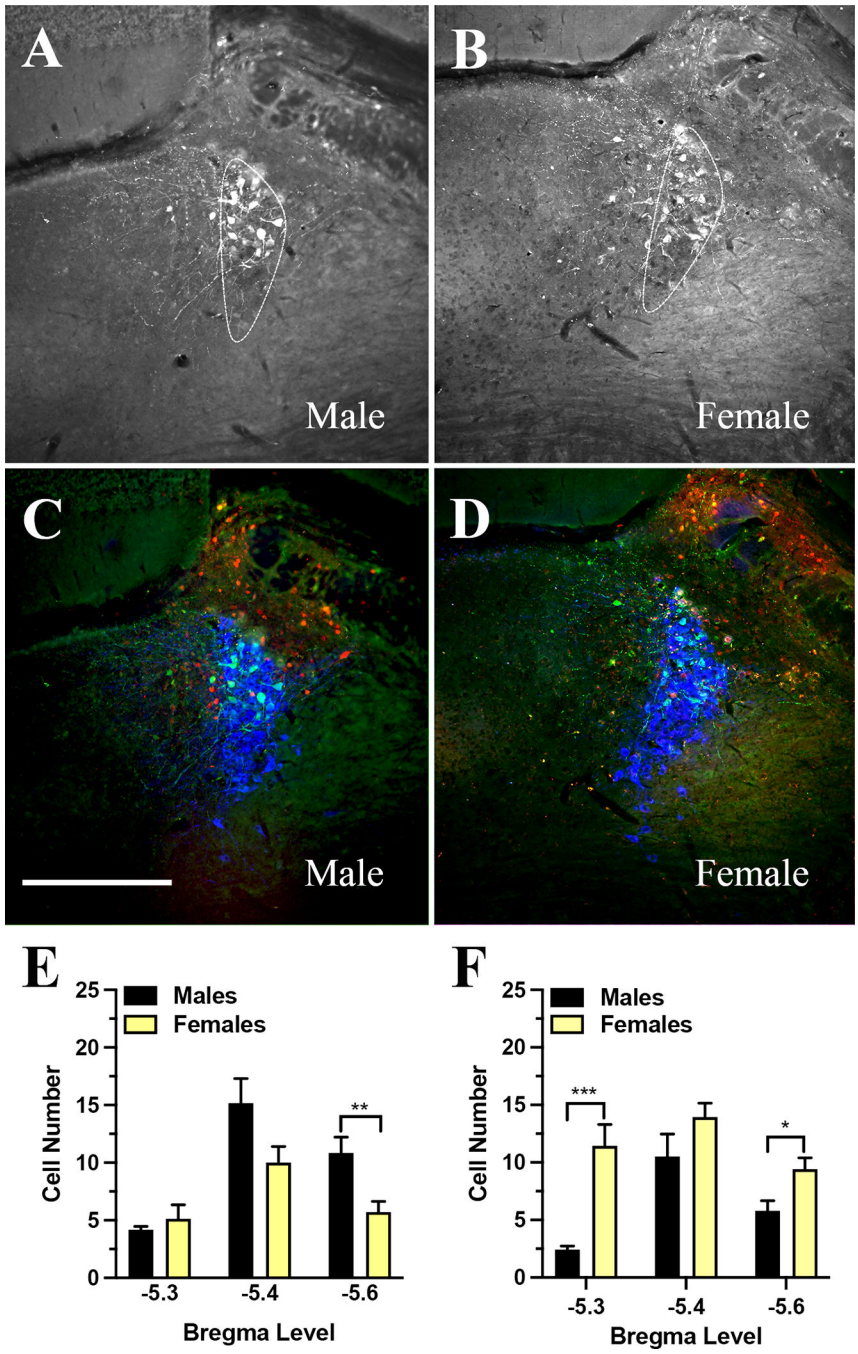

Figure 7: Innervation pattern of LC neurons and the neurons in the pericerulеus area by the mPFC efferents in male and female mice as detected by post-synaptic labeling using anterograde delivery of cre-recombinase.

Panels **A** and **B** show the distribution of green EGFP expressing cells in a male **(A)** and female **(B)** mouse brain; the LC borders are outlined by a white interrupted line. Panels **C** and **D** are merged images of the three channels, where the green cells express cre-driven EGFP, the red cells express the default tdTomato and the blue cells are the TH positive neurons of LC. Panel **E** shows the average number of EGFP cells that are colocalized with TH neurons in males and females at three different bregma levels. A higher number of green

cells were counted at – 5.6 mm to bregma in male mice when compared to the female mice ($P < 0.01$). Panel **F** shows the average number of EGFP cells in the periceruleus zone in males and females at three different bregma levels where the females expressed a higher number of green cells at bregma levels – 5.3 mm ($P < 0.001$) and – 5.6 mm ($P < 0.05$) when compared to their male counterparts. It is very likely that the last group of neurons are part of the LC interface that consists of inhibitory interneurons. Scale bar = 500 μm.

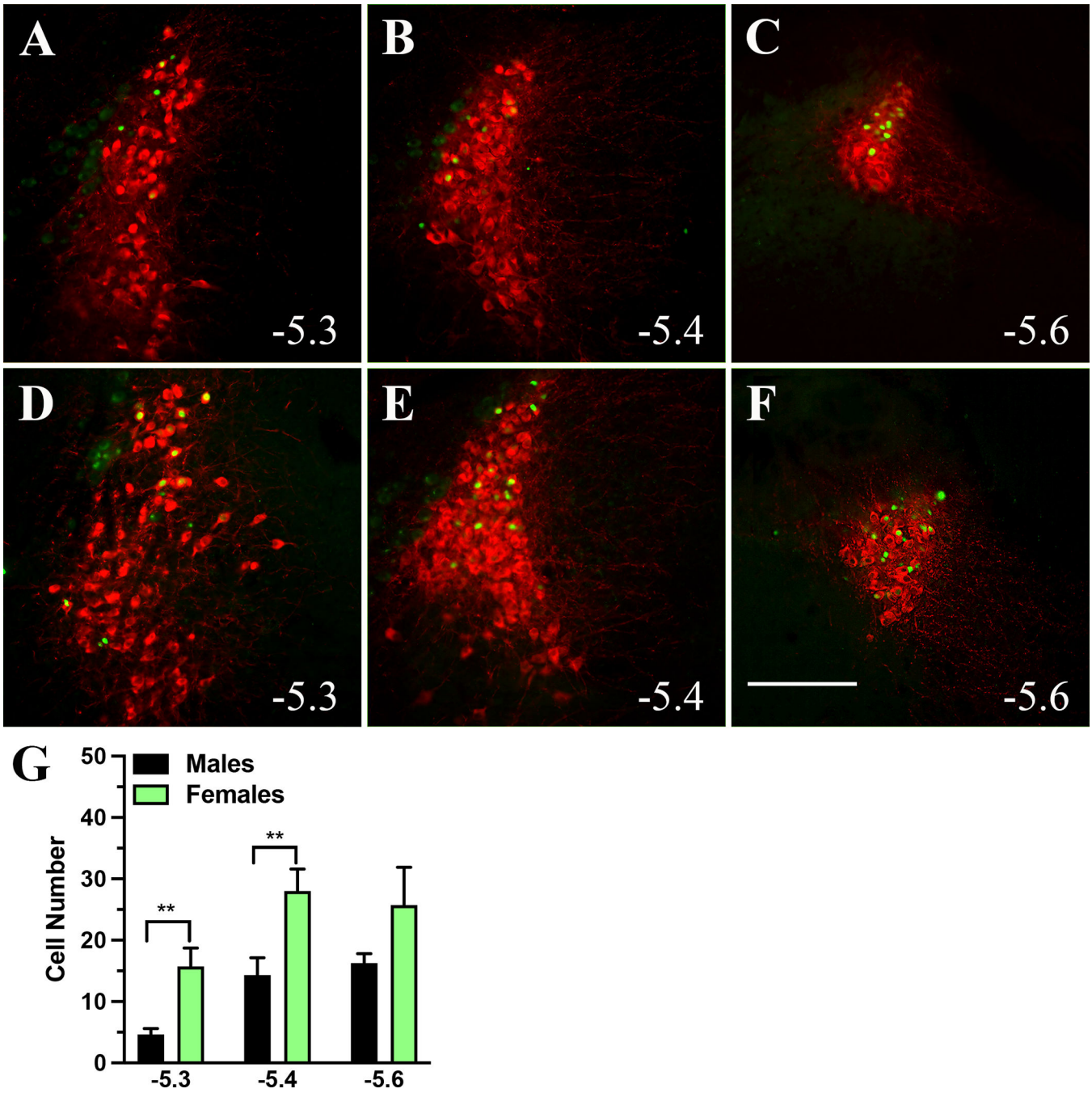

Figure 8: The distribution pattern of the LC to mPFC projections in male and female mice at three different bregma levels.

Injection of the retrograde pENN-AAV-hSyn-HI-eGFP-Cre-WPRE-SV40 virus into the mPFC labeled noradrenergic cells throughout the rostro-caudal extend of LC in male (**A** to **C**) and female (**D** to **F**) mice. The majority of retrogradely labeled cells occupied the dorsal half of the LC. The graph in panel **G** compares the projection neurons at three bregma levels, where the female mice showed a higher number of labeled neurons at – 5.3 mm (P <

0.05) and – 5.4 mm ($P < 0.05$) to bregma. The numbers on the panels indicate the corresponding bregma level (mm to bregma). Scale bar = 200 μm.